AIP Journal of Applied Physics

A study of the aftereffect of the magnetic permeability in Corich amorphous ferromagnetic alloys

P. Allia, C. Beatrice, F. Vinai, Absair T. de Rezende, and R. Sato Turtelli

Citation: Journal of Applied Physics **60**, 3258 (1986); doi: 10.1063/1.337714
View online: http://dx.doi.org/10.1063/1.337714
View Table of Contents: http://scitation.aip.org/content/aip/journal/jap/60/9?ver=pdfcov
Published by the AIP Publishing

A study of the aftereffect of the magnetic permeability in Co-rich amorphous ferromagnetic alloys

P. Allia, C. Beatrice,[a] and F. Vinai
Istituto Elettrotecnico Nazionale "Galileo Ferraris," Torino, Italy, Gruppo Nazionale di Struttura della Materia of the Consiglio Nazionale delle Ricerche, and Centro Interuniversitario di Struttura della Materia of the Ministero della Pubblica Istruzione, Torino, Italy

Absair T. de Rezende and R. Sato Turtelli
Physics Department, Universidade Estadual de Campinas, Campinas, Brazil

(Received 4 April 1986; accepted for publication 23 June 1986)

Room-temperature measurements of saturation magnetization, saturation magnetostriction, and aftereffect of the magnetic permeability have been performed on a set of Co-based amorphous ferromagnetic alloys with magnetostriction values in the range $-4\times10^{-6} \lesssim \lambda_s \lesssim +1\times10^{-6}$. The theoretical relation between aftereffect and λ_s has been verified to hold also in Co-rich amorphous alloys. The fraction of atoms participating in the ordering processes giving rise to the aftereffect is calculated to be of the order 10^{-4}. The aftereffect is shown to be related, even in these alloys, to a damping of 180° Bloch walls, whose thickness increases with decreasing λ_s. The influence of the alloy's stability on the permeability aftereffect is discussed in detail.

I. INTRODUCTION

The aftereffect of the initial magnetic permeability of Fe-rich amorphous ferromagnetic alloys is proportional at room temperature to the square of the saturation magnetostriction of the material.[1] This result has been explained by invoking the directional ordering of structural defects, interacting with the direction of the magnetization I_s through a magnetoelastic coupling.

A first version of the theory[1] predicts that the permeability aftereffect $\Delta\mu/\mu$ is directly proportional to λ_s^2, in full agreement with the experimental results for Fe-based alloys. Rather strong magnetic aftereffects were, however, also observed in near zero-magnetostriction, Co-rich amorphous alloys.[2,3] The apparent contradiction between these findings and the predictions of the magnetostrictive theory has been solved by analyzing the problem from two different viewpoints. A deeper analysis of the effect of structural distortions on the local magnetoelastic energy leads one to predict a functional dependence of the type $\Delta\mu/\mu = A + B\lambda_s^2$ for the permeability aftereffect,[4] consequently accounting in a natural way for the effects observed in zero λ_s alloys. On the other hand, additional contributions to the coupling energy between defects and magnetization have been investigated by Kronmüller *et al.*,[3,5] who pointed out that both the spin orbit and the exchange energy may be considered as possible sources of the aftereffect. A law of the type $\Delta\mu/\mu = A + B\lambda_s^2$ is derived also in this second case. Obviously, the parameters A and B are defined differently in each model. Quite unfortunately, they depend on various factors, which are sometimes not directly measurable, e.g., the number of defects responsible for the aftereffect at a given temperature. As a consequence, no quantitative comparison between the predictions of these competing models has been attempted so far.

Although the aftereffect of the magnetic permeability has been investigated in several Fe-based alloys, relatively few data for magnetostrictive, Co-rich alloys are available, since most of the measurements were specifically concerned with zero-magnetostriction ribbons.[2,3,6] In this paper a complete set of Co-based alloys (with λ_s continuously ranging from negative to positive values) is studied for the first time, in order to check experimentally the validity of the expression $\Delta\mu/\mu = A + B\lambda_s^2$ in these materials. The analysis of the behavior of the magnetic aftereffect with λ_s is helpful in determining the values of some physical parameters appearing in the theoretical expressions for $\Delta\mu/\mu$. A better knowledge of these factors could, in turn, allow one to verify if the existing approaches to the problem are based on reasonable assumptions.

II. MEASUREMENTS AND RESULTS

Room-temperature measurements of saturation magnetization, saturation magnetostriction, and low-field permeability aftereffect were performed on as-cast ribbons of composition $Co_{75}Si_5B_{20}$, $Co_{75-x}Fe_xSi_{15}B_{10}$ $(0\leqslant x\leqslant 6)$, $Co_{72}Mn_8B_{20}$, $Co_{73}B_{27}$, and $Co_{61}Fe_8Ni_{18}Cr_{3.2}Cu_2B_3Si_{4.8}$. The ribbons of the $Co_{75-x}Fe_xSi_{15}B_{10}$ alloy series were prepared at USP, São Paulo, Brazil.[7]

The saturation magnetization was measured by means of a vibrating sample magnetometer. The saturation magnetostriction was determined by using a small-angle rotation technique.[8] Both measurements were performed at UNICAMP, Campinas, Brazil. The aftereffect of the magnetic permeability was measured on similar samples at IENGF, Turin, Italy, by making use of an impulsive technique suitable to analyze the permeability decay from about 10^{-2} s after a sudden change of the domain structure of the sample.[9] $\Delta\mu/\mu \equiv \Delta B/B$ was measured at B_M at which ΔB shows a maximum in the ΔB vs B curve.[1] Examples of such a curve, for selected materials, are shown in Fig. 1.

The crystallization temperature of three samples

[a] Physics Department, Politecnico di Torino, Italy.

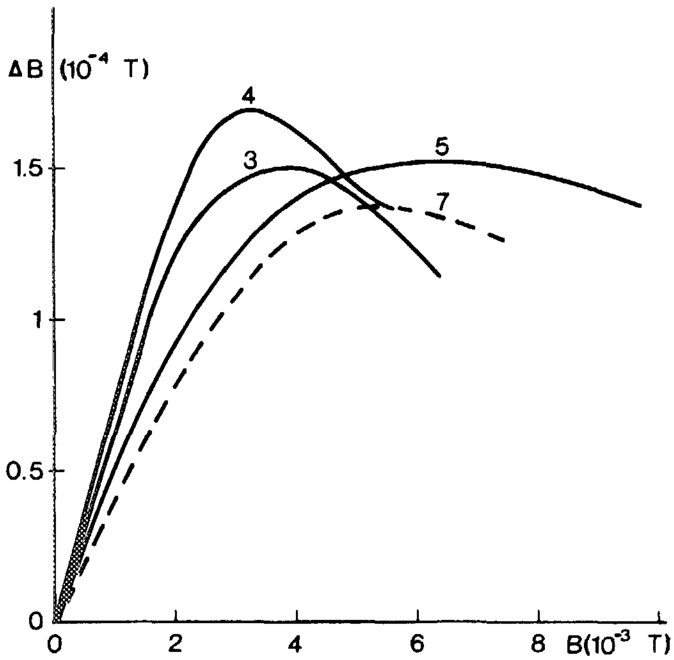

FIG. 1. Behavior of the magnetic aftereffect (ΔB) as a function of induction B in selected Co-rich amorphous alloys. Numbers refer to Table I. Full lines: negative magnetostriction; dashed line: positive magnetostriction.

($Co_{73}B_{27}$, $Co_{75}Si_5B_{20}$, $Co_{75}Si_{15}B_{10}$) was determined by a conventional DSC technique with a heating rate of 30 K/min.

The values of the saturation magnetization and of the permeability aftereffect of the considered alloys are reported in Table I, where the aftereffect is expressed, as usual,[4,10] in the more convenient form $\Delta\mu/\mu \times H_e \times I_s$, H_e being the value of the external field. The behavior of the aftereffect as a function of λ_s is shown in Fig. 2 (dots). Although some scattering is present, the experimental data are well represented by the quadratic law $\Delta\mu/\mu \times H_e \times I_s = a + b \times \lambda_s^2$, with $a = 5.67 \times 10^{-2}$ and $b = 1.05 \times 10^{10}$ J/m^3 (dashed line in Fig. 2). This result confirms the validity of the theoretical predictions also for these Co-based alloys, as far as the functional dependence of $\Delta\mu/\mu$ on λ_s is concerned. The position of the maximum of the ΔB vs B curve (B_M) for the $Co_{75-x}Fe_xSi_{15}B_{10}$ alloy series is reported in Fig. 3 as a function of λ_s. B_M is found to increase with decreasing magnetostriction (in absolute value).

III. DISCUSSION

A. Dependence of the aftereffect on the alloy's magnetostriction

The expression of the magnetic aftereffect of magnetostrictive nature is, in the light of the more recent calculations,[4]

$$\frac{\Delta\mu}{\mu} H_e I_s = 2.55 \frac{3}{32} \frac{N_T}{kT} [G(t_1) - G(t_2)] \lambda_{\text{eff}}^2 \langle \tau^2 \rangle, \qquad (1)$$

where N_T is the total number (per cubic meter) of atoms present in structural defects ordering at the temperature T, $G(t)$ is a monotonically decreasing function time,[1] t_1 and t_2 are the fixed limits of the time interval chosen to measure the aftereffect, and $\langle \tau^2 \rangle$ is the second moment of the shear-stress fluctuations according to the definition proposed by Egami *et al.*[11] The "effective" magnetostriction λ_{eff} is defined as

$$\lambda_{\text{eff}}^2 = (1/25)[8\pi\lambda_s^2 + (1/2\pi)\langle m \rangle \lambda_g^2], \qquad (2)$$

where λ_s is the saturation magnetostriction, and the constant λ_g, related to λ_s, is expressed in terms of a particular combination of the local anisotropy energy and its space derivative, as discussed elsewhere.[4] Finally, $\langle m \rangle$ is the average value of a bond-orientational order parameter describing the degree of distortion of elementary cells in a metallic glass.[12]

The measurable parameters appearing in the right-hand side of Eq. (1) are T, $G(t_{1,2})$, and λ_s. Both $\langle \tau^2 \rangle$ and $\langle m \rangle$

TABLE I. Saturation magnetostriction and permeability aftereffect values for the studied Co-rich alloys (Nos. 1–9). Representative data for Fe-based alloys (Nos. 10–15) are reported for comparison.

No.	Material (nominal composition)	λ_s (10^{-6})	$(\Delta\mu/\mu) H_e \times I_s$ (10^{-1} J/m^3)
1	$Co_{73}B_{27}$	−3.7	2.96
2	$Co_{75}Si_5B_{20}$	−3.9	2.15
3	$Co_{75}Si_{15}B_{10}$	−3.7	1.05
4	$Co_{73}Fe_2Si_{15}B_{10}$	−2.7	1.08
5	$Co_{71}Fe_4Si_{15}B_{10}$	−0.6	0.49
6	$Co_{70.4}Fe_{4.6}Si_{15}B_{10}$	+0.2	0.27
7	$Co_{69}Fe_6Si_{15}B_{10}$	+1.0	0.67
8	$Co_{72}Mn_8B_{20}$	−2.5	1.60
9	$Fe_{7.9}Co_{61.1}Ni_{18.1}Cr_{3.2}Cu_2B_{3.1}Si_{4.6}$	+0.4	0.97
10	$Fe_{29}Ni_{49}P_{14}B_6Si_2$[a]	4.3	0.09
11	$Fe_{40}Ni_{40}P_{14}B_6$[a]	8.7	0.41
12	$Fe_{80.8}Cr_5B_{14.2}$[a]	14.4	1.34
13	$Fe_{75}Cr_{4.8}B_{20.2}$[a]	14.8	2.00
14	$Fe_{80}W_3B_{17}$[a]	15.9	2.17
15	$Fe_{40}Ni_{38}Mo_4B_{18}$[a]	16.1	1.66

[a] P. Allia and F. Vinai, Phys. Rev. B **26**, 422 (1986).

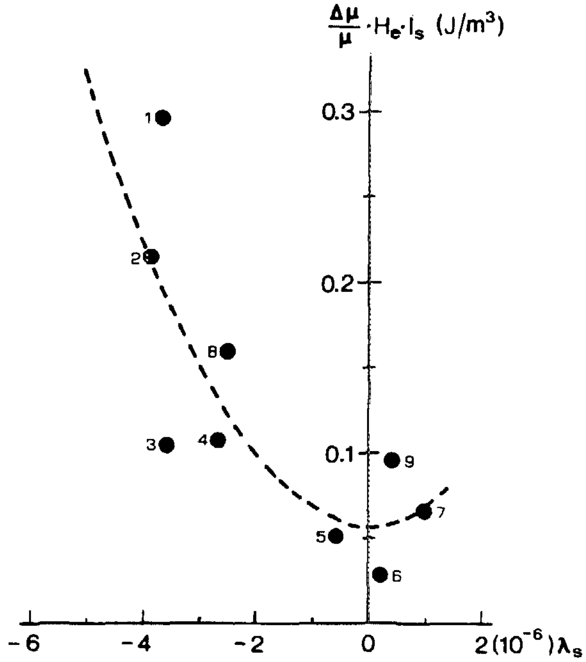

FIG. 2. Plot of the permeability aftereffect $(\Delta\mu/\mu)H_e \times I_s$ as a function of magnetostriction of Co-rich alloys. Alloys identified as in Table I. Full lines: best-fit curve, $(\Delta\mu/\mu)H_e \times I_s = 5.67\times 10^{-2} + 1.05\times 10^{10}\lambda_s^2$.

may be estimated from a simulation of the structure of an amorphous metal. For instance, $\langle \tau^2 \rangle^{1/2} = 3.29$ eV/Å^3 $= 5.26\times 10^{-18}$ J/atom, and $\langle m \rangle = 0.013$ in the realistic model proposed by Egami and Srolovitz.[13] In our opinion, such values are representative of both quantities for the set of amorphous alloys considered here. The parameters λ_g and N_T may be obtained from the analysis of the present experimental data. Since we need just an order-of-magnitude estimate of these quantities, we make here the simplifying assumption that N_T is the same in each alloy, and that λ_g remains substantially a constant for small changes of λ_s near $\lambda_s = 0$. It is known, in fact, that λ_g retains a positive value even when $\lambda_s \rightarrow 0$.[4] Further considerations about N_T are made in Sec. III B. From Eqs. (1) and (2), and from the experimental data, we have:

$$(\Delta\mu/\mu)H_e I_s = a + b\lambda_s^2,$$

$$a = 2.55\,\frac{3}{32}\,\frac{N_T}{kT}\,[G(t_1) - G(t_2)]\,\frac{1}{25}\,\frac{1}{2\pi}\,\langle m\rangle \lambda_g^2 \langle \tau^2\rangle$$

$$= 5.67\times 10^{-2}\ \mathrm{J/m^3},$$

$$b = 2.55\,\frac{3}{32}\,\frac{N_T}{kT}\,[G(t_1) - G(t_2)]\,\frac{1}{25}\,8\pi\langle \tau^2\rangle$$

$$= 1.05\times 10^{10}\ \mathrm{J/m^3}. \qquad (3)$$

As a consequence,

$$\lambda_g = (4\pi\sqrt{a/b}/\sqrt{\langle m\rangle}) = 2.56\times 10^{-4}, \qquad (4)$$

$$N_T = 13.9(kT/\langle \tau^2\rangle)b \simeq 2.2\times 10^{25}$$

atoms/m^3 (at room temperature).

In other words, the atoms participating in the ordering processes which give rise to the aftereffect are a fraction $\sim 10^{-4}$ of the total number ($\approx 10^{29}$ atoms/m^3).

This result is quite reasonable. Together with the hypothesis that each structural defect involves—on the average, a small number of atoms (10–50)[1,11]—this value of N_T supports the usual picture of localized ordering events, randomly distributed in the material and weakly correlated.

The value of λ_g is rather large, if compared with the magnetostriction of these alloys, not exceeding 5×10^{-6} in absolute value. This result is again reasonable, since λ_g is expected to be much greater than λ_s.[4]

It may be interesting to make a comparison between the present aftereffect data, and the ones obtained on as-cast Fe-

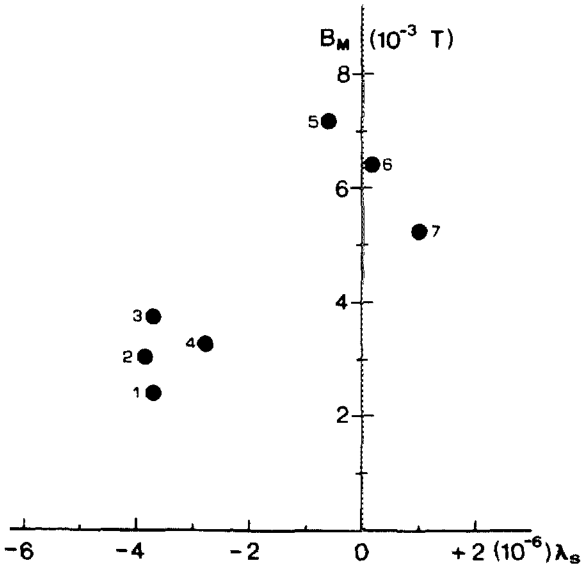

FIG. 3. Position of the maximum of the $\Delta B(B)$ curves as a function of λ_s in the Co–Fe–Si–B alloy series. Alloys identified as in Table I.

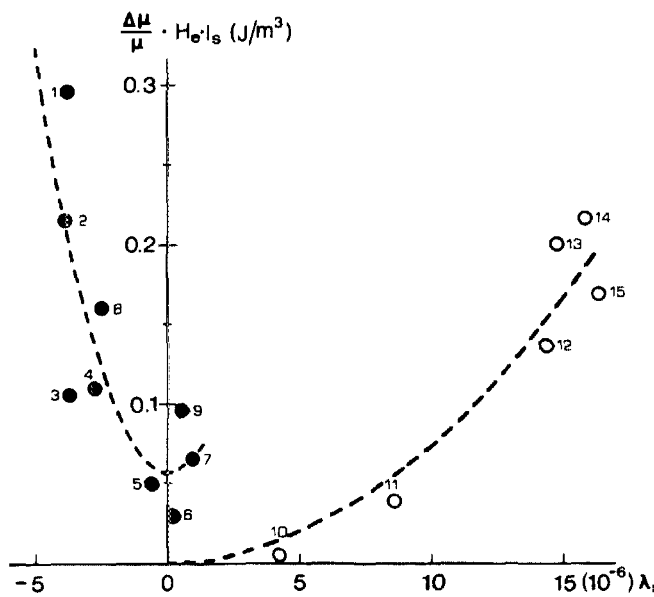

FIG. 4. Behavior of the permeability aftereffect with magnetostriction in the Co-rich alloy series (full dots) and in some representative Fe-rich alloys (open dots), in the magnetostriction interval $-5\times 10^{-6} \lesssim \lambda_s \lesssim +15\times 10^{-6}$. Alloys identified as in Table I. Lines: best-fit curves, $(\Delta\mu/\mu)\times H_e \times I_s = 5.67\times 10^{-2} + 1.05\times 10^{10}\times \lambda_s^2$ and $(\Delta\mu/\mu)\times H_e \times I_s = 7.3\times 10^{8}\times \lambda_s^2$, respectively.

based alloys with low (positive) magnetostriction, taken from Ref. 4. The measuring technique was exactly the same for both series. The $\Delta\mu/\mu H_e \times I_s$ vs λ_s curves of Co- and Fe-rich alloys are shown in Fig. 4 in the range $-5\times10^{-6} \lesssim \lambda_s \lesssim +15\times10^{-6}$. The full line is the best-fit curve determined from the whole Fe-based alloy series $\Delta\mu/\mu\times H_e\times I_s = 7.3\times10^8 \lambda_s^2$.[4] The possibility of grouping Fe- and Co-rich alloys in two distinct families is strikingly confirmed by these data. Notice that the slope of the best-fit quadratic law is over one order of magnitude larger in Co-based alloys than in Fe-based ones. The origin of such a discrepancy is presently not clear. In light of the magnetostrictive model, it could be attributed to a difference of some structural parameters ($N_T, \langle m\rangle, \langle\tau^2\rangle$) between the two alloy families.

B. Dependence of the aftereffect on the alloy's stability

Although the reported aftereffect data are well represented by the quadratic law discussed in Sec. III A, some scattering is still present. The reasons for this scattering are investigated here. As a matter of fact, the intensity of $\Delta\mu/\mu\times H_e\times I_s$ at a given temperature turns out to be related not only to the alloy's magnetostriction but also to N_T, the number of atoms participating in the ordering processes which give rise to the aftereffect [see Eq. (1)]. This number, of the order $\approx 10^{25}$ atoms/m^3, may vary as a consequence of changes of the structural state of the amorphous alloy. This effect is particularly evident after structural relaxation, as discussed elsewhere.[4,10]

Generally speaking, N_T is significantly affected by the stability of the alloy. This fact is not surprising, since the ordering processes responsible for the aftereffect take place easier in less stable structures. A convincing proof of this statement may be given by analyzing the behavior of $\Delta\mu/\mu\times H_e\times I_s$ in materials having the same λ_s and different thermal stability. This condition occurs in three of the considered alloys, precisely $Co_{73}B_{27}$, $Co_{75}Si_5B_{20}$, and $Co_{75}Si_{15}B_{10}$, characterized by close magnetostriction values and different crystallization temperature T_x. In these alloys, T_x is increased and $\Delta\mu/\mu\times H_e\times I_s$ is reduced by addition of Si, as shown in Table II.

These considerations allow one to conclude that the intensity of the aftereffect may be influenced almost independently by λ_s and N_T. When both parameters are allowed to vary from one alloy to another, the aftereffect data appear to be rather scattered when plotted versus λ_s (see Fig. 2). When λ_s is kept fixed, the effect of pure variations of the stability (and N_T) is enhanced (alloys 1–3 in Fig. 2). On the other hand, when the thermal stability of a set of alloys is kept as constant as possible (e.g., by varying the transition metal content without changing the metalloid ratio, as in the $Co_{75-x}Fe_xSi_{15}B_{10}$ series[7]), the influence of the magnetostriction on the aftereffect intensity is dominant, and the scattering is reduced (alloys 3–7 in Fig. 2). Finally, it should be mentioned that N_T may also be changed by varying the quenching rate at which the ribbons are produced. As a matter of fact, $\Delta\mu/\mu\times H_e\times I_s$ increases with increasing the quenching rate. This effect has been discussed in different papers.[14,15]

TABLE II. Permeability aftereffect and crystallization temperatures of three Co-based alloys having similar magnetostriction values.

No.	Material (nominal composition)	$(\Delta\mu/\mu)H_eI_s$ (10^{-1} J/m^3)	T_x (K)
1	$Co_{73}B_{27}$	2.96	718
2	$Co_{75}Si_5B_{20}$	2.15	765
3	$Co_{75}Si_{15}B_{10}$	1.05	777

C. Dependence of Bloch wall thickness on magnetostriction

According to Néel's theory,[16] the behavior of the magnetic aftereffect (ΔB) as a function of induction B gives information about the type and the thickness of the Bloch walls, whose motion is progressively hindered by the magnetic viscosity. No direct Kerr-effect observation of the magnetic domain structures was possible on the narrow ribbons under consideration. The presence of a maximum in the ΔB vs B curve (see Fig. 1) suggests, however, that in these alloys the measured aftereffect is substantially related to a damping of the motion of 180° walls.[16] This result is not surprising, at least in ribbons with $\lambda_s > 0$, where the magnetic domain pattern is primarily composed of domains separated by 180° walls. In ribbons with $\lambda_s \lesssim 0$, the actual domain structure may be very different, owing to the presence of a transverse anisotropy and complicated secondary domain structures.[17] However, the shape of the ΔB vs B curves (Fig. 1, full lines) is similar to the one observed in ribbons with positive magnetostriction (dashed line in Fig. 1), indicating that even in this case the aftereffect is mainly related to 180° wall motion. The position of the maximum of the ΔB vs B curve B_M is proportional to the wall thickness δ, corresponding to a wall displacement of about $0.45\times\delta/2$.[18] Without a direct knowledge of the average distance between walls, it is not possible to convert the measured B_M values into actual wall displacements. However, it is clear from Fig. 3 that in the whole $Co_{75-x}Fe_xSi_{15}B_{10}$ series B_M increases with decreasing λ_s. This result is most probably related to a decrease of the anisotropy energy of magnetostrictive type, and to the consequent increase of the wall thickness parameter $\delta = \pi(A/K_{\rm eff})^{1/2}$,[19] where A is the exchange energy coefficient, and $K_{\rm eff}$ the (total) residual anisotropy energy. A variation of δ could also be attributed, in principle, to changes of A; however, the Curie temperatures of this alloy series[7] indicate that the variations of A with varying Fe content do not justify, by themselves, the systematic variation of δ with λ_s.

The present aftereffect measurements suggest that the wall thickness increases by a factor of 3 with a reduction of λ_s from 3.7×10^{-6} to 6×10^{-7}. More precise information about the wall thickness in these alloys could be obtained through aftereffect measurements performed on larger ribbons, where the simultaneous observation of the domain structure should be easier.

IV. CONCLUSIONS

A quadratic relation between the magnetic permeability aftereffect and the saturation magnetostriction has been observed also in Co-rich amorphous alloys. The results are in good agreement with the theoretical predictions. The experimental data allow one to obtain a reasonable value for N_T, the number of atoms involved in ordering processes responsible for magnetic aftereffects in amorphous materials. The room-temperature intensity of the aftereffect has been shown to depend critically on both the alloy's magnetostriction and N_T. This circumstance explains the scattering typically observed in the plots of the aftereffect as a function of λ_s.

The pure effect of magnetostriction on $\Delta\mu/\mu$ may be completely disentangled from the one of N_T only in measurements performed on amorphous ribbons having comparable thermal stability, and produced with similar quenching rates.

Additional information on the functional dependence of the aftereffect on the magnetostriction could be obtained by preparing, with such prescriptions, new ribbons on the $Co_{75-x}Fe_xSi_{15}B_{10}$ family, having higher Fe content. In this way, the functional relation between aftereffect and magnetostriction could also be checked in the positive magnetostriction side of this alloy series.

ACKNOWLEDGMENTS

The authors would like to thank Professor F. P. Missell of USP, São Paulo, Brazil for supplying the samples of the Co–Fe–Si–B series. This work has been performed within the agreement for scientific cooperation between Italy's CNR and Brazil's CNPq.

[1] P. Allia and F. Vinai, Phys. Rev. B **26**, 6141 (1982).
[2] T. Jagielinski, J. Appl. Phys. **53**, 2282 (1982).
[3] H. Kronmüller, N. Moser, and F. Rettenmeier, IEEE Trans. Magn. **MAG-20**, 1388 (1984).
[4] P. Allia and F. Vinai, Phys. Rev. B **33**, 422 (1986).
[5] H. Kronmüller, Phys. Status Solidi B **127**, 131 (1985).
[6] T. Jagielinski, J. Appl. Phys. **53**, 7852 (1982).
[7] A. D. Santos, A. M. Severino, and F. P. Missell, J. Magn. Magn. Mater. (to be published).
[8] K. Narita, J. Yamasaki, and H. Fukunaga, IEEE Trans. Magn. **MAG-16**, 435 (1980).
[9] P. Allia, P. Mazzetti, G. P. Soardo, and F. Vinai, J. Magn. Magn. Mater. **19**, 281 (1980).
[10] P. Allia, R. Sato Turtelli, F. Vinai, and A. Lovas, Solid State Commun. **47**, 951 (1983).
[11] T. Egami, K. Maeda, and V. Vitek, Philos. Mag. A **41**, 883 (1980).
[12] P. Allia and F. Vinai, J. Phys. **46**, C8-317 (1985).
[13] T. Egami and D. Srolovitz, J. Phys. F **12**, 2141 (1982).
[14] P. Allia, F. E. Luborsky, R. Sato Turtelli, G. P. Soardo, and F. Vinai, IEEE Trans. Magn. **MAG-17**, 2615 (1981).
[15] P. Allia, G. Riontino, R. Sato Turtelli, and F. Vinai, Solid State Commun. **43**, 821 (1982).
[16] L. Néel, J. Phys. Rad. (Paris) **13**, 249 (1952).
[17] C. Aroca, J. M. Riveiro, G. Rivero, and M. C. Sanchez, J. Magn. Magn. Mater. **15-18**, 1379 (1980).
[18] P. Allia and F. Vinai, IEEE Trans Magn. **MAG-17**, 1481 (1981).
[19] H. Kronmüller, J. Phys. (Paris) **41**, C8-618 (1980).